Investigating catalytic de-oxygenation of cellulose, xylan and lignin bio-oils using HZSM-5 and Fe-HZSM-5

Chetna Mohabeer, Luis Reyès, Lokmane Abdelouahed, Stéphane Marcotte, Bechara Taouk

Investigating catalytic de-oxygenation of cellulose, xylan and lignin using HZSM-5 and Fe-HZSM-5

Chetna Mohabeer[a], Luis Reyes[a], Lokmane Abdelouahed[a], Stéphane Marcotte[b], Bechara Taouk[a,*]

[a] Normandie Univ, INSA Rouen Normandie, UNIROUEN, Laboratoire de Sécurité des Procédés Chimiques, LSPC EA-4704, 76000 Rouen, France

[b] Normandie Univ, INSA Rouen Normandie, UNIROUEN, COBRA UMR-6014, 76000 Rouen, France

[*] bechara.taouk@insa-rouen.fr

Abstract

This study presents a detailed analysis of the liquid and gaseous pyrolytic products of the three principal components of biomass (cellulose, hemicellulose and lignin) using two different catalysts (HZSM-5 and its iron-modification, Fe-HZSM-5). The experiments were conducted in a semi-batch reactor under the same operating conditions for all feed materials. The results allow the determination of the provenance of aromatic compounds, which are essential components of bio-oil to be used as a bio-fuel. Transformation schemes have been proposed for each biomass component so as to better comprehend the formation of these aromatic compounds. BET specific surface area, BJH pore size distribution and FT-IR technologies have been used to characterise the catalysts, while gas chromatography-mass spectrometry (GC-MS), flame ionisation detection (GC-FID) and thermal conductivity detection (GC-TCD) were used to examine the liquid and gaseous pyrolytic products. It was firstly found that HZSM-5 favoured the decarbonylation route (production of CO), whilst Fe-HZSM-5 favoured the decarboxylation one (production of CO_2) for the same feed. Then, a competition was seen to arise from the presence of the catalysts: the chemical family present in majority in the oils was the one converted by the catalysts, rather than one single family. Finally, from the transformation schemes, it was seen that even though both catalysts boosted the aromatics production, HZSM-5 produced more aromatics than its iron-modification. It was also observed that HZSM-5 formed more phenols, and hence, more coke, than Fe-HZSM-5.

Keywords: Pyrolysis, woody biomass components, catalytic de-oxygenation, de-oxygenation schemes

1. Introduction

The aromatic compounds benzene, toluene and xylenes are often grouped together as BTX [1]. They are bulk chemicals which are vital for the petrochemical industry, namely for transportation fuels. However, these aromatics have a negative environmental impact given that they are produced from fossil resources in an energy intensive process. It is thus important to find sustainable options to produce BTX. One such option is using biomass as feedstock in a process such as catalytic pyrolysis, using catalysts to de-oxygenate the produced oil. It should be noted that biomass comprises of three major components: cellulose, hemicellulose and lignin. Investigating the catalytic pyrolysis of the latter components can help in better comprehending how this process works.

Zhou *et al*. [2] have studied the catalytic pyrolysis of cellulose with different zeolites in a TG-FTIR setup from 30 to 800 °C under a 30 mL/min N_2 flow. They have found that HZSM-5 was the most efficient catalyst in terms of de-oxygenation degree as it improved the conversion of oxygenated families like esters, aldehydes and acids into aromatics. About the same observations were made by Lei *et al*. [3], who used a Py-GC/MS setup with temperatures ranging from 150 to 700 °C. Guo *et al*. [4] investigated the catalytic pyrolysis of xylan-based hemicellulose in a TG-FTIR setup from 30 to 350 °C under 30 mL/min N_2 using different zeolites (HZSM-5, H-*β* and USY). They found that all of the zeolites had a significant effect on the de-oxygenation of xylan, and that HZSM-5, along with having good de-oxygenation efficiency, suppressed the formation of char residues. Zhu *et al*. [5], on their part, performed experiments in a pyroprobe with temperatures between 350 and 900 °C. They found that metal-modified HZSM-5 (Fe and Zn) was even more efficient than the parent zeolite concerning de-oxygenation activity. Lignin de-oxygenation was examined by Zhan *et al*. [6] in a μ-pyrolysis reactor using an array of catalysts (HZSM-5, MCM-41, TiO_2, ZrO_2 and Mg(Al)O) at 400, 500 and 600 °C using He as carrier gas. They found that HZSM-5 was the most efficient catalyst in forming aromatics; the highest yield obtained was at 600°C, the highest temperature they used.

Now, concerning the pyrolytic conversion schemes of chemical families involved in catalytic pyrolysis, several studies tackling one or arbitrary compounds have indeed been reported in literature [7]–[10]. To report on some of the relevant data previously published in literature, Gayubo *et al*. [11] investigated on the pyrolytic conversion of alcohols and phenols using HZSM-5. They found that the dehydration process gave rise to propene from alcohols, which later produced hydrocarbons. They also noted a very low conversion rate of phenols. Guaiacols were found to form aromatics by decarboxylation, along with a carbonaceous material deposited within the catalyst matrix. In another study [12], it was observed that aldehydes converted to C_{6+} olefins, albeit with a low conversion rate; ketones produced alkenes via dehydration followed by decarboxylation and decarbonylation; acids and esters, having the same reactivities, gave rise to ketones, which later decomposed as mentioned above. Finally, they found that levoglucosan formed furans, which degraded further to give aromatics, olefins, CO, CO_2, water and coke.

However, to the best of our knowledge, no study undertook detailed analysis of the pyrolytic products of the three woody biomass components in a single setup, under the same operating conditions. This study aims to shed some light on the mechanisms of BTX production from the catalytic pyrolysis of cellulose, hemicellulose and lignin so as to better understand their provenance. This can help in optimising their production from the catalytic pyrolysis of biomass. This study is a direct follow-up of previous research led by our group on the same raw materials [13].

2. Experimental section

2.1 Materials used and elemental analyses

The bio-polymers were utilised in their pure form: microcrystalline cellulose having a density of 1.5 g/cm^3 at 20 °C was purchased from Merck (Ref. 1.02330.0500-500G) while xylan, which was used as proxy for hemicellulose as the latter is not commercialised in its original form, was of corn stover origin. Xylan was bought from Tokyo Chemical Company Co. Ltd. (Ref. X0078-100G). Finally, the lignin used was “alkali lignin” or “Kraft lignin” obtained from Sigma-Aldrich (Ref. 471003-100G). This type of

lignin might not completely represent the behaviour of native lignin in biomass, but, it was chosen based on its frequent use in literature [14]–[18] so as to acquire some information about the products of pyrolysis and de-oxygenation of native lignin. **Tables 1** and **2** show the ultimate and the proximate analyses of all raw materials used in this study. The total C, H and N were measured on samples using a CHN elemental analyser Flash 2000 (Thermofisher Scientific) while the proximate analysis was conducted by using TGA experiments, based on Garcia *et al.* [19]. A detailed mineral analysis was conducted on the biomass components samples used for this study. The complete results can be found in the supplementary materials (**Table A-1**).

Table 1: Ultimate analysis of the different biomass components

Biomass/Biomass	**Elemental analysis (wt. %)**			
Component used	Carbon	Hydrogen	Nitrogen	Oxygen
Cellulose	41.74	6.08	<0.01	52.18
Xylan	41.47	6.48	<0.01	52.05
Lignin	57.04	4.76	<0.01	38.21

Table 2: Proximate analysis of different biomass components based on TGA experiments (wt. %)

	Moisture content	**Volatile matter**	**Fixed carbon**	**Ash**
Cellulose	4.61	91.87	3.51	<0.01
Hemicellulose	4.66	76.80	18.31	0.23
Lignin	11.28	60.38	22.31	6.03

2.2 Catalysts preparation and characterisation

2.2.1 Catalysts preparation

2.2.1.1 HZSM-5

The catalyst [hydrophobic HZSM-5 catalyst in its proton form (H^+)] was acquired from ACS materials in the form of pellets. The SiO_2/Al_2O_3 ratio was 38, the specific surface area about 250 g/m^2 and the

pore size about 5 Å. The catalyst was triturated and sieved between 1.0 and 1.4 mm. The apparent porosity of this catalyst was calculated by a method described in the supplementary materials and was found to be 0.61. The dried catalyst was introduced in a tubular furnace to be calcined at a temperature of 550 °C during 4 hours [20] at atmospheric pressure, with a heating rate of 2 °C/min.

2.2.1.2 Fe-HZSM-5

The previously mentioned catalyst, HZSM-5, was used as a support for synthesis by impregnation of Fe-HZSM-5. An iron nitrate salt, ferric (III) nitrate 9-hydrate ($Fe(NO_3)_3.9H_2O$), was purchased from PanReac AppliChem. For each 10 g of HZSM-5, 4.04 g of the iron nitrate salt were diluted in 100 mL of deionized water [20]. The catalyst was impregnated by the ferric solution, agitated and heated at 80 °C for 10 minutes. The catalyst was then dried overnight in an oven at a temperature of 105 °C. The dried catalyst then underwent the same calcination programme described previously. The apparent porosity was 0.61 for Fe-HZSM-5.

2.2.2 Catalyst characterisation methods

2.2.2.1 Specific surface area and pore size distribution

BET surface area was measured by nitrogen adsorption at -196 °C in a Quanta Sorb Junior apparatus (Ankerschmidt). Before analysis, the samples were degassed for 30 min at 200 °C. Each measurement was repeated three times and an average value was taken.

Nitrogen adsorption-desorption isotherms were obtained on a Micromeritics TRISTAR 3000 analyser at -196 °C over a wide relative pressure range from 0.01 to 0.995. The samples were degassed under vacuum for several hours before nitrogen adsorption measurements. The pore diameter and the pore size distribution were determined by the Barret–Joyner–Halenda (BJH) method using the adsorption branch of isotherms.

2.2.2.2 Surface acidity

The acidity of the catalysts was measured by infrared spectroscopy of adsorbed pyridine. It has been demonstrated in literature that pyridine is the probe molecule of choice to examine the acidity of zeolites as used in biomass pyrolysis applications [21]. To investigate the nature of acid sites and bonding of sulphate ions on the surface of catalysts, FT-IR (Spectrum BX, Perkin-Elmer) spectra were obtained in the range of 600-4000 cm^{-1}. The samples for acidity measurement were prepared in powder form, then saturated with small amount of pyridine, and degassed at 100 °C for one hour. The FTIR spectra in absorbance mode after the pyridine treatment were subtracted with those of the untreated catalysts to obtain the peaks only due to pyridine–acid interactions [22].

2.3 Pyrolysis experimental and analytical setup

2.3.1 Pyrolysis setup

The pyrolysis runs were done in a semi-continuous experimental set up. It comprised of a quartz reactor with a special configuration, as illustrated by **Figure 1**. The total length was 1050 mm. The reactor included two zones: a pyrolysis zone (ϕ= 56 mm and L = 760 mm) and a catalysis zone (ϕ= 26 mm and L = 290 mm). Both zones were placed horizontally in a tubular furnace. A stainless steel "spoon" could be inserted at the reactor inlet and the other end was connected to a condenser and a flask, placed inside a cold bath to recover the bio-oils formed from the condensation of pyrolytic vapours. The flask was connected to a sampling bag, in which the non-condensable gases were collected to be later analysed. A flowmeter, placed near the mouth of the reactor, allowed the regulation of the flow of nitrogen, used as carrier gas. The cold bath and the refrigerant were both kept at a constant temperature of -10 °C.

The pyrolysis experiments were conducted at temperature of 500 °C using a flow rate of 500 mL/min of nitrogen for each raw material used. About 3 g of raw materials were placed onto the spoon, which was kept near the mouth of the reactor. For the experiments comprising the catalysts, a catalyst-to-biomass ratio of 4:1 was used. The vapour residence time through the catalyst bed was calculated to be about 3 s. After the reaction, the non-condensable gases were recovered in the

sampling bag and the setup was finally left to cool so as to permit the collection of the solid char. The oil was recovered by using acetone with 99.98% purity, with a known added amount of nonane, used as internal standard.

2.3.2 Pyrolytic products analysis methods

2.3.2.1 GC-MS analysis

The liquid product analysis methods have previously been detailed in Mohabeer *et al*. [13]. The analysis of the recovered bio-oil was performed using a gas chromatograph-mass spectrometer instrument GC-MS (Varian 3900 - Saturn 2100T). The analysed components were identified with Varian WS (WorskStation) and NIST 2002 software by comparing the mass spectrum obtained to mass spectra from the NIST library. Kovats retention indices of the identified peaks were then calculated and compared to reference values for confirmation of their identity.

2.3.2.2 GC-FID analysis

Once the identity of the peaks was confirmed, a flame ionisation detector (FID), GC-FID Scion 456-GC Bruker instrument, was used to quantify the components. The compounds obtained were then grouped into chemical “families”, each having the same main functional group.

2.3.2.3 GC analysis of non-condensable products

The analysis of the non-condensable gases was performed with a gas chromatograph instrument from Perkin Elmer, Clarus 580, equipped with two detectors, a FID and a thermal conductivity detector (TCD). The instrument also comprised of a Shincarbon St 100 120 column, a methaniser and a hydrogen generator. The oven was regulated from 100-200 °C. The carrier gas was argon. The TCD was used to determine the components such as H_2 and N_2. The FID detected the carbonated components, except for CO and CO_2, which were detected with the help of the methaniser.

2.3.2.4 Karl Fischer (KF) titration method

Volumetric KF titrations were performed with a Metrohm 870 KF TitrinoPlus apparatus. An aqualine sodium tartrate solution was used as titrating agent, along with Hydranal Composite 5 and Hydranal Methanol Rapid as working media. The sample weight used was in the range of 0.17-0.20 g.

3. Results

3.1 Catalyst characterisation

The values obtained for the specific surface area of the catalysts used were 286 m^2/g for HZSM-5 and 221 m^2/g for Fe-HZSM-5. It can be seen that the BET surface area decreased after the iron modification, but remained relatively high. As for the pore size distribution, from the isotherms, it was seen that HZSM-5, along with the modified version, exhibited mostly microporous structures. It was also seen that while the microporous volume did not change significantly for both catalysts (0.15 cm^3/g), the pore specific volume did incur a change: 0.41 cm^3/g for HZSM-5 and 0.25 cm^3/g for Fe-HZSM-5, pointing that some pores were occupied by Fe ions.

Infrared is the most powerful technique for the study of zeolite acidity [22]. Zeolites are known to possess two kinds of acidities. Firstly, for zeolites in the H-form, the hydroxyl groups linking Si and Al atoms are said to have strong Brønsted acid properties. Then, Lewis acid sites are usually associated with extra-framework Al and O species [23]. The stepwise desorption of the two catalysts used was performed at 100, 150, 200, 300 and 400 °C. **Figure 2** shows the spectra obtained at 150 and 400 °C. The figure for HZSM-5 clearly demonstrates the presence of bands at 1436 and 1580 cm^{-1}, characteristic of Brønsted acid sites, as well as bands at 1482 and 1596 cm^{-1}, representing Lewis acid sites [24]. The principal effect of the iron modification can be observed as a decrease in the acid bands. However, only the bands at 1482 and 1596 cm^{-1} were completely removed, providing evidence that Lewis acid sites were occupied by Fe.

3.2 Effect of catalyst use on pyrolytic product distributions

The pyrolysis of the three biomass components at 500°C with and without any catalytic treatment yielded different product distributions. It should be noted that values exceeding 95 % were obtained for all mass balances conducted, and all were brought to 100 %. The results obtained have been illustrated in **Figure 3**, from which it can clearly be seen that the most significant amount of bio-oil came from the pyrolysis of xylan and cellulose, with79 wt. % and 77 wt. %, respectively. The largest quantity of non-condensable gases was produced by cellulose pyrolysis (about 12 wt. %), while that of lignin yielded more char than any other component, approximately 57 wt. %. Now, even though xylan seemed to give rise to more liquid than the other two biomass components, it should be noted that cellulose is present in a higher fraction in biomass; hence, it can be said that cellulose contributed most in liquid and gas production. These experiments provided the product distribution of the pyrolysis of the three biomass components as conducted in a semi-batch reactor, under the same operational conditions; and this provided the base of our study.

The use of catalysts had a significant impact on the product distribution of the biomass components. Concerning cellulose and xylan, the use of the zeolites increased gas production, while impeding that of bio-oil. Also, as can be seen from **Figure 4**, the oxygen content of the bio-oils (oxygen present in humidity notwithstanding) was quite impacted by the use of the catalysts. This result seems to indicate that certain oxygenated compounds present in the pyrolytic vapours were de-oxygenated in the presence of the catalysts to form more gaseous (CO, CO_2 and H_2) and water molecules. The only exception was the lignin bio-oil, where the difference in oxygen content was insignificant. This may be explained by the fact that the major part of lignin (57 wt. %) remained unconverted, and so, no important change was observed. Also, a table listing the water content of the different bio-oils can be found in the supplementary materials (**Table A-2**). It could be seen that HZSM-5 tended to favour the formation of water, and hence, the dehydration reaction, for all the biomass components as compared to the iron-modified catalyst.

3.3 Effect of catalyst use on bio-oil and non-condensable gas composition

The percentages of the different chemical families present in the bio-oils recovered and those of the various components present in the non-condensable gases are listed in **Tables 3** and **4**. It is clearly shown by the results obtained that without any catalytic treatment, the major part of carboxylic acids present in the bio-oils came from xylan and lignin (24.68 mol. % and 14.01 mol. %, respectively) while the bio-oil from cellulose mainly comprised of carbohydrates (42.84 mol. %). Concerning the effect of catalyst use on the oxygen content of the bio-oil, **Figure 4** showed that Fe-HZSM-5 and HZSM-5 had about the same efficiency in terms of de-oxygenation; the use of both catalysts reduced the oxygen content of cellulose and xylan quite significantly.

Table 3: Composition (mol. %) of chemical families present in bio-oils

Chemical groups in bio-oil	mol. %								
	Cellulose			Xylan			Lignin		
	No catalyst	HZSM-5	Fe-HZSM-5	No catalyst	HZSM-5	Fe-HZSM-5	No catalyst	HZSM-5	Fe-HZSM-5
Carboxylic acids	7.04	-	2.12	24.68	2.31	-	14.01	-	-
Alkanes	0.60	0.53	-	7.39	-	-	9.68	14.61	100
Aromatics	4.76	26.62	23.18	3.58	16.08	15.08	10.00	-	-
Alcohols	8.44	22.35	10.09	17.13	6.77	8.18	-	-	-
Aldehydes	5.58	1.21	1.81	3.46	2.06	0.77	-	-	-
Amides	2.93	2.02	1.54	8.43	1.10	1.82	5.84	15.09	-
Ketones	11.19	4.74	9.61	10.61	9.57	10.82	6.07	9.12	-
Esters	4.46	1.73	1.50	8.54	0.63	3.12	-	-	-
Furans	0.56	2.76	4.64	2.27	4.17	5.58	-	-	-
Guaiacols	-	-	-	1.19	2.12	1.56	6.75	26.05	-
Phenols	11.63	38.05	45.51	9.91	55.19	53.07	47.66	35.13	-

Carbohydrates	42.84	-	-	2.82	-	-	-	-	-

Table 4: Composition (vol. %) of components present in non-condensable gases

Non-condensable gases components	**vol. %**								
	Cellulose			**Xylan (hemicellulose)**			**Lignin**		
	No catalyst	HZSM-5	Fe-HZSM-5	No catalyst	HZSM-5	Fe-HZSM-5	No catalyst	HZSM-5	Fe-HZSM-5
H_2	1.60	1.38	17.61	1.60	0.90	13.92	15.56	15.67	7.99
CO	54.80	61.43	38.68	46.59	60.16	40.00	9.54	11.39	7.85
CO_2	34.27	23.66	33.63	43.78	24.98	34.49	59.97	58.67	64.35
CH_4	3.67	2.74	2.45	5.37	2.47	2.83	11.35	12.27	18.36
C_2H_4	2.59	6.20	4.45	1.42	6.29	4.84	0.34	0.99	0.75
C_2H_6	0.66	0.38	0.27	0.99	0.40	0.34	3.23	0.82	0.70
C_3H_6	1.79	4.21	2.90	-	4.79	3.57	-	0.04	-

An interesting point is that even though the same catalysts were used with respect to the three biomass components, not the same families were impacted. For instance, de-oxygenation efficiency notwithstanding, in the case of cellulose pyrolysis, the use of both catalysts resulted in reducing the carbohydrates percentage. On the other hand, for xylan, the use of the catalysts brought down the carboxylic acids percentage. The same phenomenon was noted with lignin, where the catalyst activity affected the phenols percentage. This observation led to the conclusion that a "competition" existed within the chemical families present; the catalysts mainly targeted the group present in a higher percentage in the bio-oil.

To better compare the different results obtained when utilising the catalysts, the conversion and production rates of the different chemical families in the bio-oils, and those of the non-condensable gas components were used as reference. The calculations done to obtain these values have been presented in the supplementary materials. These values have been tabulated in **Tables 5** and **6**. Also, **Figure 5** illustrates the evolution of the percentages of the major chemical families for each bio-oil sample with and without catalyst use. It can be seen (from **Figure 5**) that the above-mentioned observation holds true: the evolution of the same chemical group varied for each biomass component.

Table 5: Conversion and production rates of chemical families present in bio-oils

Chemical families	**Conversion rate (-%) and production rate (+%)**					
	Cellulose + HZSM-5	**Cellulose + Fe-HZSM-5**	**Xylan + HZSM-5**	**Xylan + Fe-HZSM-5**	**Lignin + HZSM-5**	**Lignin + Fe-HZSM-5**
Carboxylic acids	-100	-90	-95	-100	-100	-100
Alkanes	-43	-100	-100	-100	-3	-9
Aromatics	+257	+61	+130	+5	-100	-100
Alcohols	+69	-61	-80	-88	No change	No change

Aldehydes	-86	-89	-70	-94	No change	No change
Amides	-56	-83	-93	-95	+67	-100
Ketones	-73	-72	-54	-75	-3	-100
Esters	-75	-89	-96	-91	No change	No change
Furans	+215	+174	-6	-39	No change	No change
Guaiacols	No change	No change	-9	-67	+149	-100
Phenols	+109	+29	+185	+34	-52	-100
Carbohydrates	-100	-100	-100	-100	No change	No change

Table 6: Conversion and production rates of non-condensable gas components

Non-condensable gases components	**Conversion rate (-%) and production rate (+%)**					
	Cellulose + HZSM-5	**Cellulose + Fe-HZSM-5**	**Xylan + HZSM-5**	**Xylan + Fe-HZSM-5**	**Lignin + HZSM-5**	**Lignin + Fe-HZSM-5**
H_2	+114	+3261	+103	+4364	+1	-39
CO	+185	+121	+366	+340	+20	-2
CO_2	+75	+208	+106	+304	-2	+28
CH_4	+90	+110	+66	+170	+9	+93
C_2H_2	No change	No change	No change	No change	No change	No change
C_2H_4	+508	+439	+1494	+1644	+191	+160
C_2H_6	+48	+28	+46	+75	-75	-74
C_3H_4	-100	-100	-84	-89	No change	No change
C_3H_6	+495	+406	Production	Production	Production	No change
C_3H_8	-100	-100	No change	No change	Production	No change

Now, Mullen and Boateng [25] presented the possibility that phenol formation was inhibited by the addition of Fe on an HZSM-5 support; this statement can be confirmed by our observations. From

Tables 5 and **6,** it can be observed that HZSM-5 had a more pronounced selectivity towards phenol production as compared to Fe-HZSM-5 (HZSM-5: +109 % for cellulose and +185 % for xylan vs. Fe-HZSM-5: +29 % for cellulose and +34 % for xylan). Another observation that was noted was that the addition of Fe suppressed the formation of aromatics; HZSM-5 had a higher production rate than its iron-modification when it came to aromatics (122 % more for cellulose and 119 % more for xylan).

3.3.1 Effect of catalyst on products of cellulose pyrolysis

If the results obtained for cellulose are examined, it can be seen that there was a complete reduction of carbohydrates with both HZSM-5 (-100 %) and Fe-HZSM-5 (-100 %). However, it could be seen that the use of HZSM-5 resulted in a high production of aromatics (+257 %), but also some oxygenated chemical families like furans and phenols; meanwhile, the use of Fe-HZSM-5 did lead to the formation of phenols and furans, but, the percentages produced were much lower, while the aromatics formation was less significant (+61 %). This difference is explained when the conversion rates of the gaseous components are analysed: the production rates of H_2 and CO_2 were noticeably higher with Fe-HZSM-5 than with HZSM-5. These observations can prompt the supposition that the use of Fe-HZSM-5 favoured the production of gas molecules over other oxygenated liquid components and water molecules.

3.3.2 Effect of catalyst on products of xylan pyrolysis

There were a few noticeable differences between the data obtained for the pyrolysis of xylan without and with catalytic treatment and those for cellulose. These differences are logical and can be explained by the different structures of cellulose and xylan [26]. An important observation is that while almost carbohydrates were converted by the use of catalysts for cellulose, for xylan, the carboxylic acid group was the one targeted by the catalysts. Almost complete reduction was achieved by using both catalysts (-95 % with HZSM-5 and -100 % with Fe-HZSM-5). Now, the difference in product distribution when utilising the two catalysts could be seen in the products formed by the catalytic activity: for HZSM-5, the end product was mainly phenols and aromatics, with a less

significant formation of gas molecules like CO and C_2H_4, while for the iron-modified catalyst, only an important production of the gas molecules H_2, CO, CO_2 and C_2H_4 was observed, strengthening the previously-drawn observation about the catalytic activity of Fe-HZSM-5, and contradicting the findings of Zhu *et al*. [5].

3.3.3 Effect of catalyst on products of lignin pyrolysis

The behaviour of lignin was completely different from those of cellulose and xylan. Again, this observation can be explained by the differences in the structures of the three biomass components [26]. However, in this case, there was absolutely no correlation in the catalytic behaviour. Phenols were found to be the major family present in the lignin bio-oil and they were indeed impacted by the use of the catalysts (-52 % for HZSM-5 and -100 % for Fe-HZSM-5); it should be noted nonetheless that a very low liquid yield was obtained from lignin (57 wt. % was recovered as solid residue). What could be observed from this part was that at an operating temperature of 500 °C, lignin pyrolysis with catalytic treatment did not contribute in the liquid fraction. It should however not be forgotten that the extraction method used to separate lignin from a biomass, the interactive forces that exist between the three biomass components when they are intertwined and the presence of minerals influence greatly the behaviour of the said lignin. Hence, the native lignin might present a different behaviour.

3.4 Further discussion

Concerning the evolution of non-condensable gas molecules, an interesting observation was made pertaining to the CO and CO_2 emitted with the use of the catalysts. The gas percentages have been illustrated in **Figure 6**. However, the percentages themselves can be misleading for, from **Table 6**, it can be seen that while the use of HZSM-5 did boost the production of CO for all three biomass components (+185 %, +366 % and +20 % for cellulose, xylan and lignin, respectively), that of Fe-HZSM-5 privileged the production of CO_2 (+208 %, +304 % and +28 % for cellulose, xylan and lignin,

respectively). From these observations, it can be inferred that the use of HZSM-5 privileged the decarbonylation route over decarboxylation one, while the opposite can be said for Fe-HZSM-5.

Comparing the different production and conversion rates investigated during the course of the study enabled the proposal of the conversion schemes for different chemical families. The proposals put forward are illustrated in this part. “Model molecules”, that is, the most abundant molecule present in each family, were taken to represent each chemical group; a detailed list of these molecules can be found in the supplementary materials (**Table A-3**). Conversion schemes have only been proposed for the major chemical families in each bio-oil sample from three biomass components.

In the case of cellulose, the major family were carbohydrates and the main compound found was levoglucosan. The conversion schemes obtained when using HZSM-5 and its iron-modification have been illustrated in **Figure 7 (a)** and **(b)**. From the latter figures, it can be seen that the common molecule formed following the activities of both catalysts is a furan. This observation is coherent in the light of studies led by Mullen and Boateng [27]: levoglucosan underwent dehydration to form furans, then through decarboxylation to produce aromatics, olefins, CO, CO_2, water and coke. However, from our results, it was apparent that decarbonylation, not decarboxylation, was predominant in the HZSM-5 activity (formation of CO), while decarboxylation was predominant in that of Fe-HZSM-5 (production of CO_2). Another difference noted was the production of hydrogen gas; the utilisation of the iron-modified zeolite seemed to enhance significantly the production of hydrogen in the non-condensable gases.

In the same manner as above, the schemes for the conversion reactions of carboxylic acids with HZSM-5 and Fe-HZSM-5 have been shown in **Figure 8 (a)** and **(b)**. From the results obtained, it can be inferred by the processes of dehydration, decarbonylation and decarboxylation did take place (formation of water, CO and CO_2). However, Gayubo *et al*. [28] have stipulated that acids underwent catalytic de-oxygenation to produce ketones first, which further degraded into alkenes. Our observations did not corroborate this statement as our results showed that along with alkenes

(C_3H_6), other products like unoxygenated aromatics, phenols and other light gases were also formed. This alternate observation can be explained by the difference in vapour residence time; Gayubo *et al*. [28] having used a residence time shorter than the one used in this study. Hence, no intermediate products (ketones, in this case) were seen during our experiments.

Finally, the transformation scheme for the conversion of the major constituents of lignin (phenols) has been presented in **Figure 9 (a)** and **(b)**. However, it should be noted that the lignin fraction did not completely degrade under the reaction conditions; as mentioned earlier, it would take a larger range of temperatures to completely decompose lignin. Also, this transformation scheme should be taken as a tentative one as the catalytic behaviour of the lignin chosen for this study might not be completely representative of native lignin. From **Figure 9**, it can be seen that the difference between the two catalysts was the same as in the previous instances (transformation schemes for cellulose and xylan); HZSM-5 favoured decarbonylation and formation of guaiacols while the iron-modified HZSM-5 gave rise to decarboxylation.

4. Conclusion

This study aimed at presenting a detailed analysis of the liquid and gaseous pyrolytic products of the three principal components of biomass (cellulose, hemicellulose and lignin) using two different catalysts (HZSM-5 and its iron-modification, Fe-HZSM-5) in the same experimental setup and under the same operating conditions. The goal was to be able to present transformation schemes for the catalytic de-oxygenation of the biomass components and thus determine the provenance of aromatic compounds in the liquid product so as to get a better idea of the composition of bio-oil to be used as a bio-fuel. It was firstly found that a “competition” arose due to the presence of a catalyst; rather than one single chemical family being targeted, the family which was present in majority was the one converted by the catalyst. Secondly, it was found that HZSM-5 tended to privilege the decarbonylation route (production of CO), whilst Fe-HZSM-5 favoured the decarboxylation one (production of CO_2) for the same feed. It was also seen that cellulose contributed most in terms of

liquid and gas molecules, while lignin gave rise to mostly solid particles. Finally, from the transformation schemes, it was seen that even though both catalysts boosted the aromatics production, HZSM-5 produced more aromatics than its iron-modification. It was also observed that HZSM-5 formed more phenols, and hence, more coke, than Fe-HZSM-5.

Acknowledgements

This project has been funded with the support from the European Union with the European Regional Development Fund (ERDF) and the Regional Council of Normandie.

References

[1] Energetics Inc., "Energy and Environmental Profile of the U.S. Chemical Industry." U.S. Department of Energy, Office of Industrial Technologies, 2000.

[2] Y. Zhou, S. Wang, X. Guo, M. Fang, and Z. Luo, "Catalytic pyrolysis of cellulose with zeolites," in *2011 World Congress on Sustainable Technologies (WCST)*, 2011, pp. 163–166.

[3] X. Lei, Y. Bi, W. Zhou, H. Chen, and J. Hu, "Catalytic Fast Pyrolysis of Cellulose by Integrating Dispersed Nickel Catalyst with HZSM-5 Zeolite," *IOP Conf. Ser. Earth Environ. Sci.*, vol. 108, no. 2, p. 022017, Jan. 2018.

[4] X. Guo, S. Wang, Y. Zhou, and Z. Luo, "Catalytic pyrolysis of xylan-based hemicellulose over zeolites," in *ResearchGate*, 2011.

[5] X. Zhu, Q. Lu, W. Li, and D. Zhang, "Fast and catalytic pyrolysis of xylan: Effects of temperature and M/HZSM-5 (M = Fe, Zn) catalysts on pyrolytic products," *Front. Energy Power Eng. China*, vol. 4, no. 3, pp. 424–429, Sep. 2010.

[6] S. Zhan *et al.*, "Py-GC/MS study of lignin pyrolysis and effect of catalysts on product distribution," *Int. J. Agric. Biol. Eng.*, vol. 10, no. 5, pp. 214–225, 2017.

[7] T. Danuthai, S. Jongpatiwut, T. Rirksomboon, S. Osuwan, and D. E. Resasco, "Conversion of methylesters to hydrocarbons over an H-ZSM5 zeolite catalyst," *Appl. Catal. Gen.*, vol. 361, no. 1, pp. 99–105, Jun. 2009.

[8] E. G. Derouane *et al.*, “Elucidation of the mechanism of conversion of methanol and ethanol to hydrocarbons on a new type of synthetic zeolite,” *J. Catal.*, vol. 53, no. 1, pp. 40–55, Jun. 1978.

[9] H. Zhang, Y.-T. Cheng, T. P. Vispute, R. Xiao, and G. W. Huber, “Catalytic conversion of biomass-derived feedstocks into olefins and aromatics with ZSM-5: the hydrogen to carbon effective ratio,” *Energy Environ. Sci.*, vol. 4, no. 6, p. 2297, 2011.

[10] J. Zhang, K. Wang, M. W. Nolte, Y. S. Choi, R. C. Brown, and B. H. Shanks, “Catalytic Deoxygenation of Bio-Oil Model Compounds over Acid–Base Bifunctional Catalysts,” *ACS Catal.*, vol. 6, no. 4, pp. 2608–2621, Apr. 2016.

[11] A. G. Gayubo, A. T. Aguayo, A. Atutxa, R. Aguado, and J. Bilbao, “Transformation of Oxygenate Components of Biomass Pyrolysis Oil on a HZSM-5 Zeolite. I. Alcohols and Phenols,” *Ind. Eng. Chem. Res.*, vol. 43, no. 11, pp. 2610–2618, May 2004.

[12] A. G. Gayubo, A. T. Aguayo, A. Atutxa, R. Aguado, M. Olazar, and J. Bilbao, “Transformation of Oxygenate Components of Biomass Pyrolysis Oil on a HZSM-5 Zeolite. II. Aldehydes, Ketones, and Acids,” *Ind. Eng. Chem. Res.*, vol. 43, no. 11, pp. 2619–2626, May 2004.

[13] C. Mohabeer, L. Abdelouahed, S. Marcotte, and B. Taouk, “Comparative analysis of pyrolytic liquid products of beech wood, flax shives and woody biomass components,” *J. Anal. Appl. Pyrolysis*, vol. 127, pp. 269–277, Sep. 2017.

[14] H. S. Choi and D. Meier, “Fast pyrolysis of Kraft lignin—Vapor cracking over various fixed-bed catalysts,” *J. Anal. Appl. Pyrolysis*, vol. 100, pp. 207–212, Mar. 2013.

[15] L. Abdelouahed, S. Leveneur, L. Vernieres-Hassimi, L. Balland, and B. Taouk, “Comparative investigation for the determination of kinetic parameters for biomass pyrolysis by thermogravimetric analysis,” *J. Therm. Anal. Calorim.*, vol. 129, no. 2, pp. 1201–1213, Aug. 2017.

[16] S. Farag, B. P. Mudraboyina, P. G. Jessop, and J. Chaouki, “Impact of the heating mechanism on the yield and composition of bio-oil from pyrolysis of kraft lignin,” *Biomass Bioenergy*, vol. 95, pp. 344–353, Dec. 2016.

[17] A. V. Maldhure and J. D. Ekhe, “Pyrolysis of purified kraft lignin in the presence of AlCl3 and ZnCl2,” *J. Environ. Chem. Eng.*, vol. 1, no. 4, pp. 844–849, Dec. 2013.

[18] H. Zhou, Y. Long, A. Meng, S. Chen, Q. Li, and Y. Zhang, “A novel method for kinetics analysis of pyrolysis of hemicellulose, cellulose, and lignin in TGA and macro-TGA,” *RSC Adv.*, vol. 5, no. 34, pp. 26509–26516, Mar. 2015.

[19] J. R. García, M. Bertero, M. Falco, and U. Sedran, “Catalytic cracking of bio-oils improved by the formation of mesopores by means of Y zeolite desilication,” *Appl. Catal. Gen.*, vol. 503, pp. 1–8, Aug. 2015.

[20] A. Aho *et al.*, “Catalytic upgrading of woody biomass derived pyrolysis vapours over iron modified zeolites in a dual-fluidized bed reactor,” *Fuel*, vol. 89, no. 8, pp. 1992–2000, Aug. 2010.

[21] R. C. Deka, “Acidity in zeolites and their characterization by different spectroscopic methods,” *Indian J. Chem. Technol.*, vol. 5, pp. 109–123, May 1998.

[22] D. Topaloğlu Yazıcı and C. Bilgiç, “Determining the surface acidic properties of solid catalysts by amine titration using Hammett indicators and FTIR-pyridine adsorption methods,” *Surf. Interface Anal.*, vol. 42, no. 6–7, pp. 959–962, Jun. 2010.

[23] J. W. Ward, “Thermal decomposition of ammonium Y zeolite,” *J. Catal.*, vol. 18, no. 3, pp. 348–351, Sep. 1970.

[24] R. W. Stevens, S. S. C. Chuang, and B. H. Davis, “In situ infrared study of pyridine adsorption/desorption dynamics over sulfated zirconia and Pt-promoted sulfated zirconia,” *Appl. Catal. Gen.*, vol. 252, no. 1, pp. 57–74, Oct. 2003.

[25] C. A. Mullen and A. A. Boateng, “Production of Aromatic Hydrocarbons via Catalytic Pyrolysis of Biomass over Fe-Modified HZSM-5 Zeolites,” *ACS Sustain. Chem. Eng.*, vol. 3, no. 7, pp. 1623–1631, Jul. 2015.

[26] P. Patwardhan, “Understanding the product distribution from biomass fast pyrolysis,” *Grad. Theses Diss.*, Jan. 2010.

[27] C. A. Mullen and A. A. Boateng, “Production of Aromatic Hydrocarbons via Catalytic Pyrolysis of Biomass over Fe-Modified HZSM-5 Zeolites,” *ACS Sustain. Chem. Eng.*, vol. 3, no. 7, pp. 1623–1631, Jul. 2015.

[28] A. G. Gayubo, A. T. Aguayo, A. Atutxa, R. Aguado, M. Olazar, and J. Bilbao, “Transformation of Oxygenate Components of Biomass Pyrolysis Oil on a HZSM-5 Zeolite. II. Aldehydes, Ketones, and Acids,” *Ind. Eng. Chem. Res.*, vol. 43, no. 11, pp. 2619–2626, May 2004.

Figure captions

Figure 1: Layout of pyrolysis reactor

Figure 2: FT-IR spectra at 150 and 400 °C for (a) HZSM-5 and (b) Fe-HZSM-5

Figure 3: Effect of catalyst use on pyrolytic product distribution (a) for cellulose, (b) for xylan, and (c) for lignin

Figure 4: Bio-oil oxygen content (mol. %)

Figure 5: Evolution of percentages (mol. %) of major chemical families in bio-oils with and without catalytic treatment

Figure 6: Evolution of percentages (vol. %) of major non-condensable gas components with and without catalytic treatment

Figure 7: Conversion scheme of the major chemical family in cellulose with (a) HZSM-5 and (b) Fe-HZSM-5

Figure 8: Conversion scheme of the major chemical family in xylan with (a) HZSM-5 and (b) Fe-HZSM-5

Figure 9: Conversion scheme of the major chemical family in lignin with (a) HZSM-5 and (b) Fe-HZSM-5

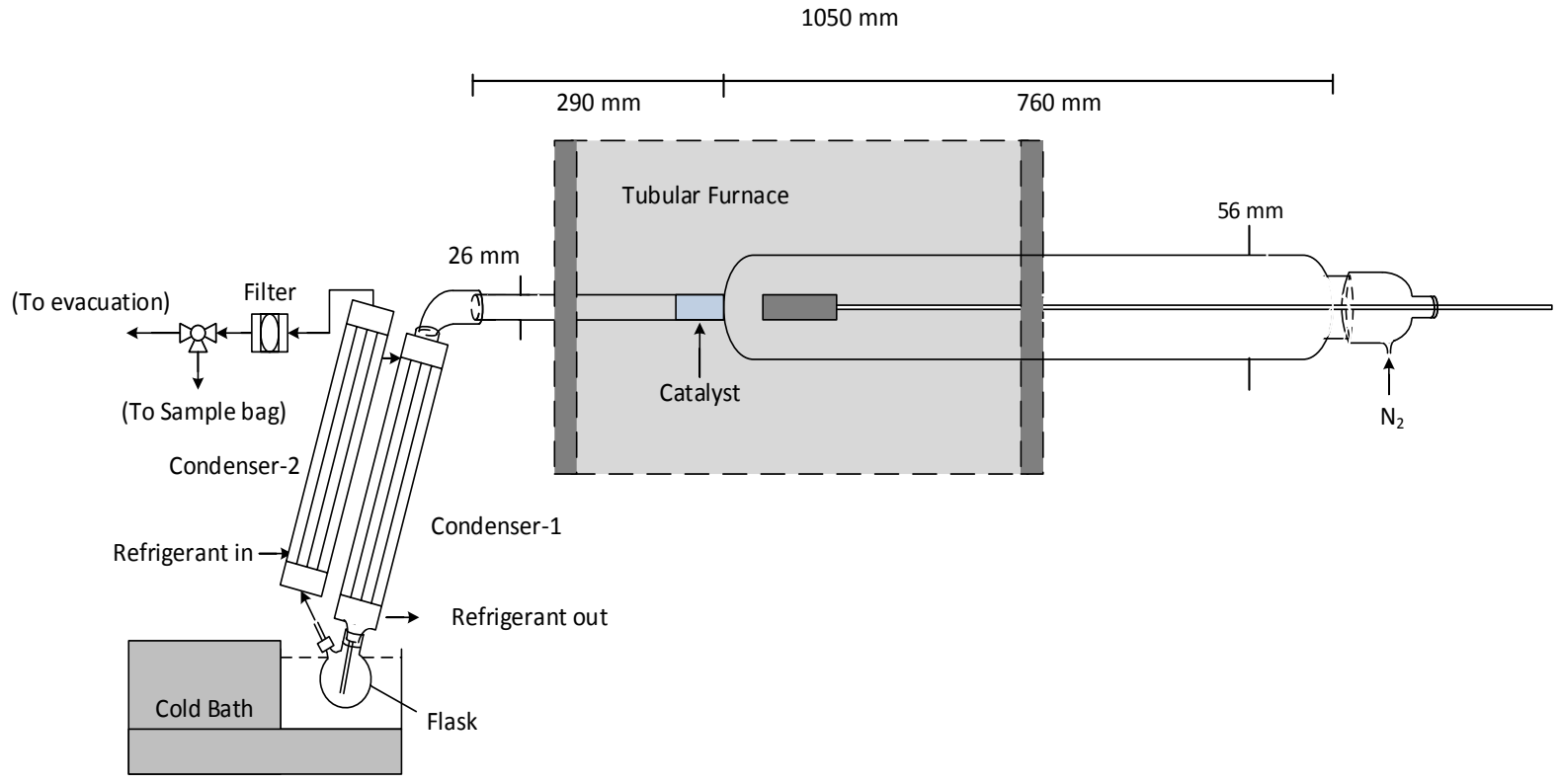
1050 mm
290 mm
760 mm
Tubular Furnace
56 mm
26 mm
(To evacuation)
Filter
(To Sample bag)
Catalyst
N_2
Condenser-2
Condenser-1
Refrigerant in
Refrigerant out
Cold Bath
Flask

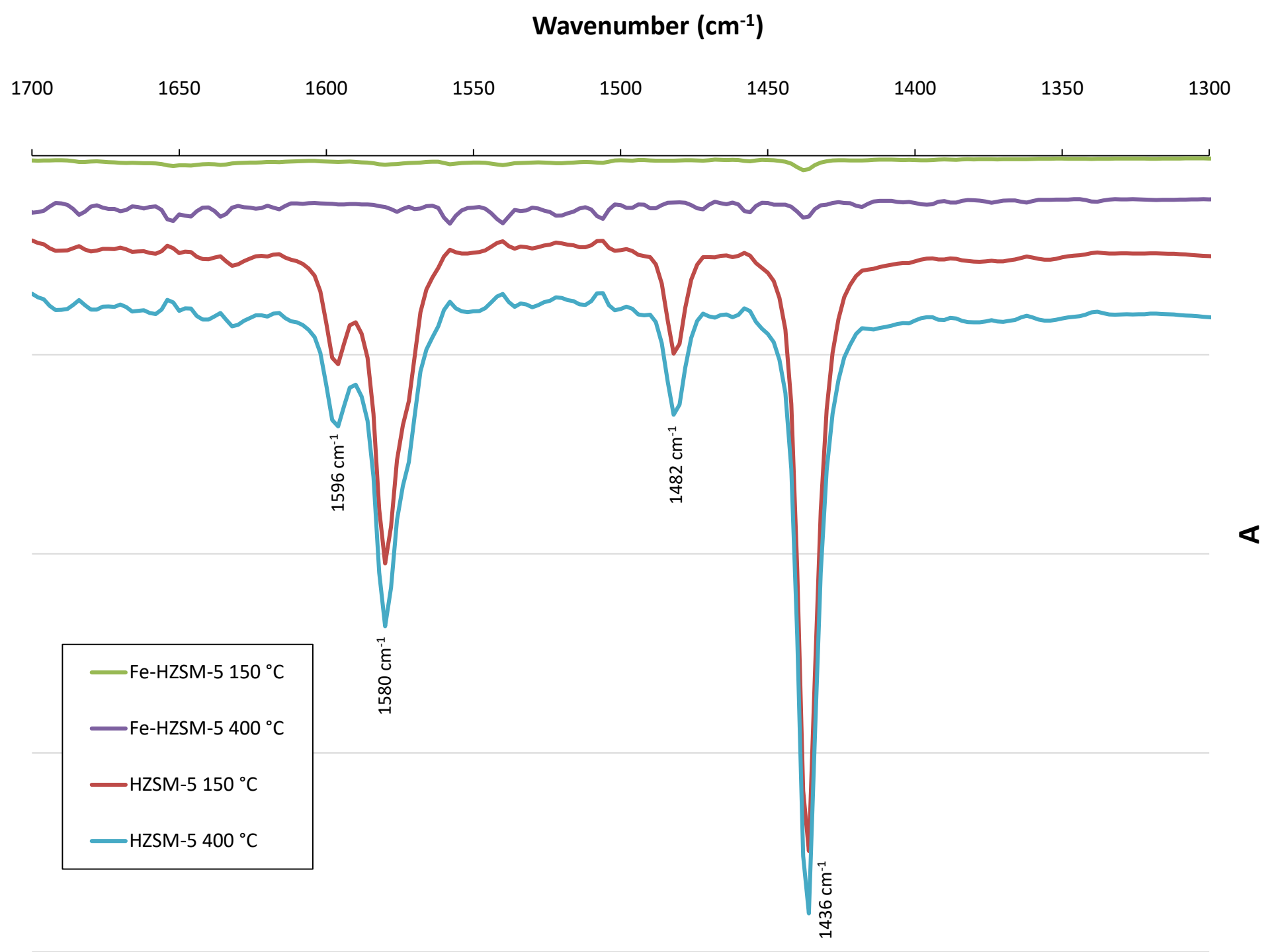
Wavenumber (cm-1)
1700
1650
1600
1550
1500
1450
1400
1350
1300
1596 cm-1
1580 cm-1
1482 cm-1
1436 cm-1
A
Fe-HZSM-5 150 °C
Fe-HZSM-5 400 °C
HZSM-5 150 °C
HZSM-5 400 °C

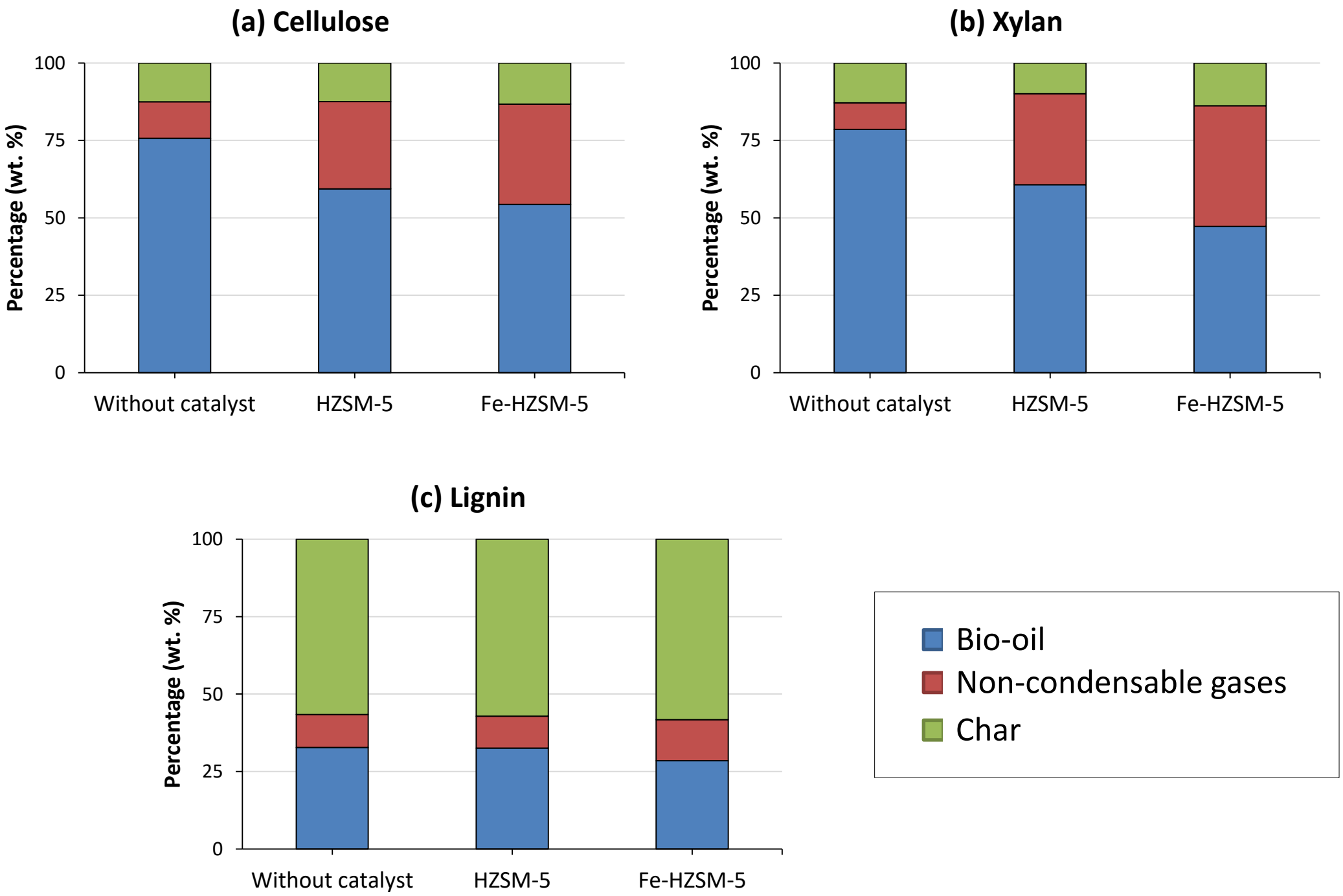
(a) Cellulose
(b) Xylan
(c) Lignin
Percentage (wt. %)
100
75
50
25
0
Without catalyst
HZSM-5
Fe-HZSM-5
Bio-oil
Non-condensable gases
Char

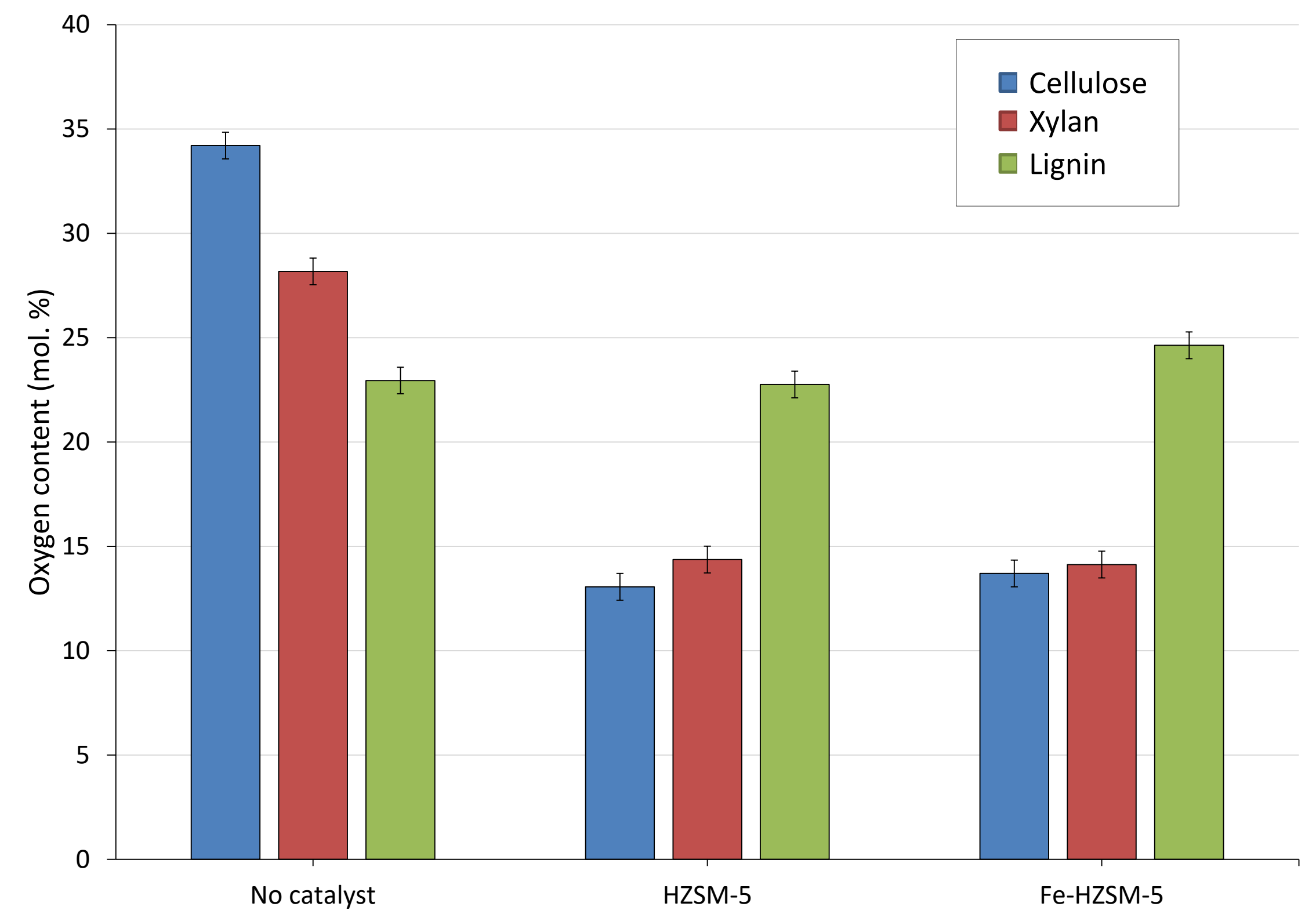
Oxygen content (mol. %)
40
35
30
25
20
15
10
5
0
Cellulose
Xylan
Lignin
No catalyst
HZSM-5
Fe-HZSM-5

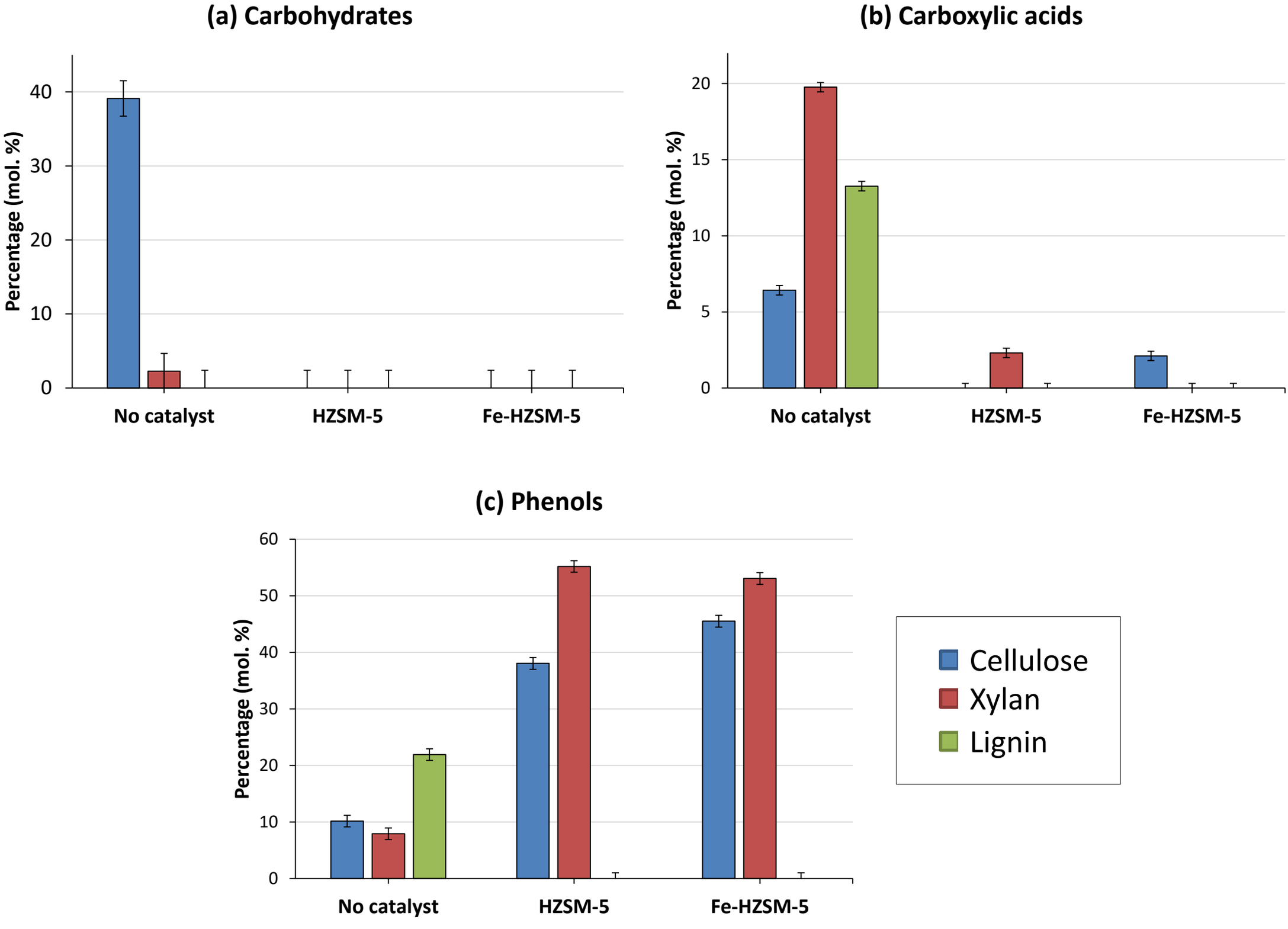
(a) Carbohydrates
Percentage (mol. %)
40
30
20
10
0
No catalyst
HZSM-5
Fe-HZSM-5
(b) Carboxylic acids
Percentage (mol. %)
20
15
10
5
0
No catalyst
HZSM-5
Fe-HZSM-5
(c) Phenols
Percentage (mol. %)
60
50
40
30
20
10
0
No catalyst
HZSM-5
Fe-HZSM-5
Cellulose
Xylan
Lignin

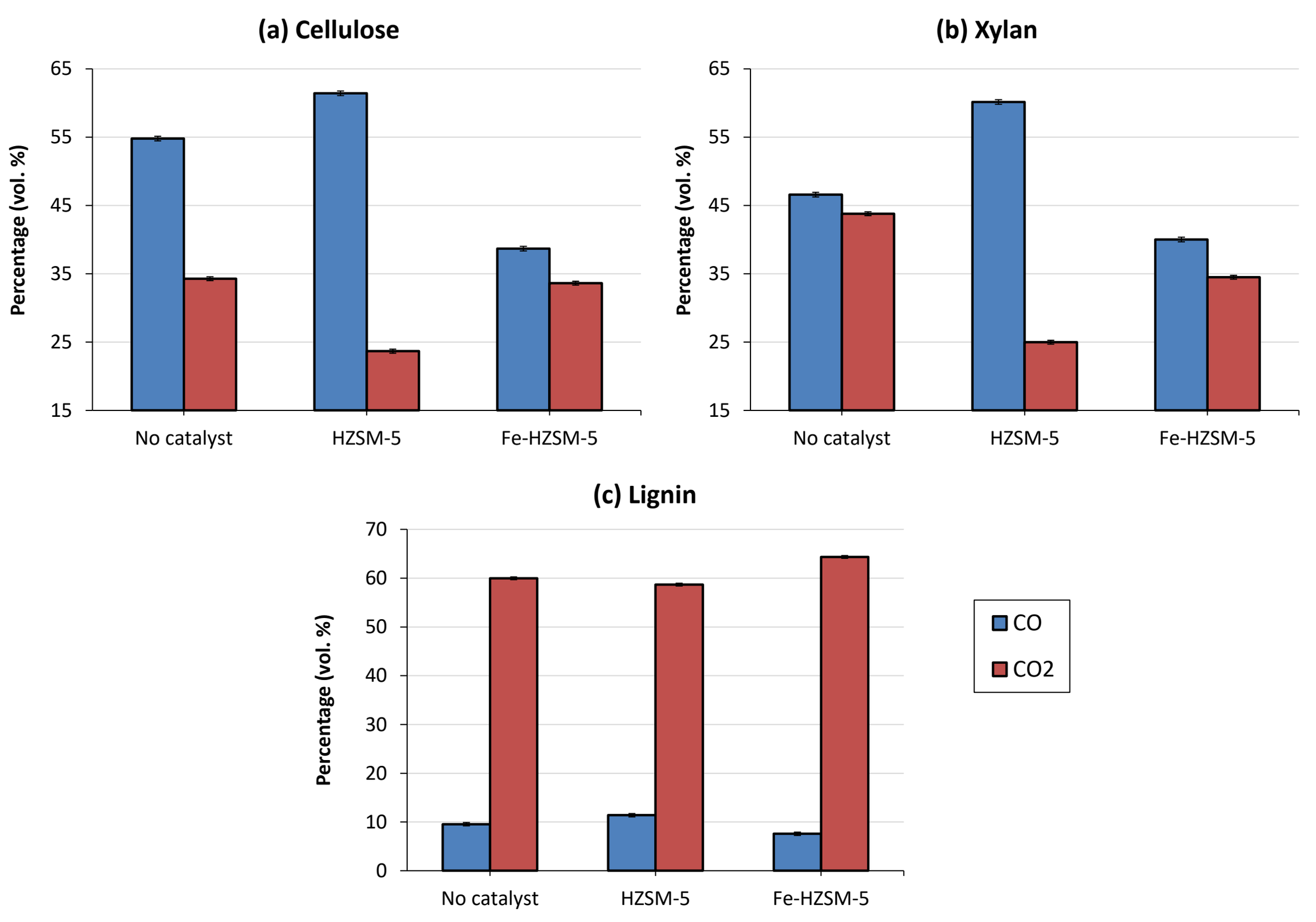
(a) Cellulose
Percentage (vol. %)
65
55
45
35
25
15
No catalyst
HZSM-5
Fe-HZSM-5
(b) Xylan
Percentage (vol. %)
65
55
45
35
25
15
No catalyst
HZSM-5
Fe-HZSM-5
(c) Lignin
Percentage (vol. %)
70
60
50
40
30
20
10
0
No catalyst
HZSM-5
Fe-HZSM-5
CO
CO2

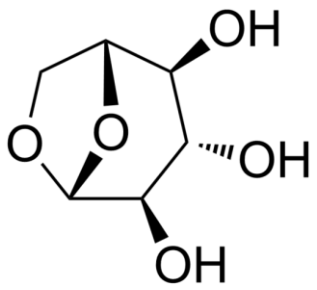

Levoglucosan
(Carbohydrates)

(a)

HZSM-5

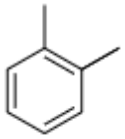

C_8H_{10} (Aromatics)

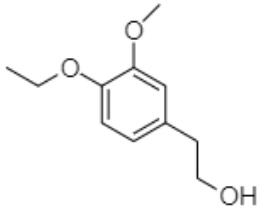

$C_{11}H_{16}O_3$ (Alcohols)

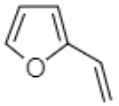

C_6H_6O (Furans)

+ CO, C_2H_4, C_3H_6, H_2O + coke

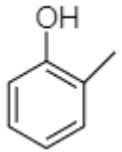

C_7H_8O (Phenols)

Fe-HZSM-5

(b)

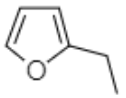

C_6H_8O (Furans)

+ H_2, CO, CO_2, CH_4, C_2H_4, C_3H_6 + coke

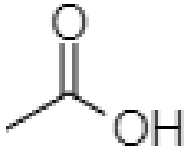

$C_2H_4O_2$
(Carboxylic acids)

HZSM-5

(a)

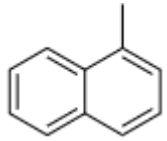

$C_{11}H_{10}$ (Aromatics)

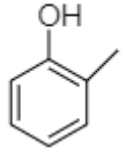

C_7H_8O (Phenols)

+ CO, C_2H_4, C_3H_6, H_2O + coke

Fe-HZSM-5

(b)

H_2, CO, CO_2, CH_4, C_2H_4, C_3H_6, + coke

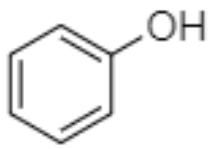

C_6H_6O
(Phenols)

(a)

HZSM-5

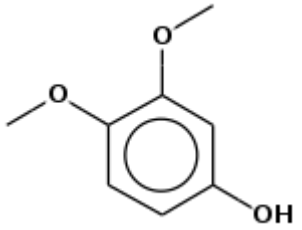

$C_8H_{10}O_3$ (Guaiacols)

+ CO, C_2H_4, H_2O + coke

Fe-HZSM-5

(b)

CO_2, CH_4, C_2H_4 + coke